



**Gesellschaft für Anlagen-
und Reaktorsicherheit
(GRS) mbH**

**Ventilation Test
at Mont Terri:
GEOELECTRIC
MONITORING**



**Gesellschaft für Anlagen-
und Reaktorsicherheit
(GRS) mbH**

**Ventilation Test
at Mont Terri:
Geoelectric Monitoring
of Opalinus Clay
Desaturation**

Tilman Rothfuchs
Lothar Hartwig
Karsten Hellwald
Michael Komischke
Rüdiger Miehe
Klaus Wiczorek

November 2004

Remark:

This report was prepared under contract No. 02 E 9501 with the Bundesministerium für Wirtschaft und Arbeit (BMWA) and under contract No. FIKW-CT-2001-00126 with the European Commission.

The work was conducted by the Gesellschaft für Anlagen- und Reaktorsicherheit (GRS) mbH.

The authors are responsible for the content of this report.

**GRS - 207
ISBN 3-931995-74-7**

Deskriptoren:

Bergbau, Deutschland, Endlager, Experiment, Frankreich, Geoelektrik, Internationale Zusammenarbeit, Kalibrierung, Labor, Langzeitsicherheit, Lüftung, Schweiz, Spanien, Überwachung

Foreword

This report presents information on geoelectric measurements performed by GRS during a Ventilation Experiment (VE) in the Mont Terri Underground Research Laboratory (MTURL).

The VE was a joint experiment performed by four partners of the Mont Terri project. The partners were the Spanish Empresa Nacional de Residuos Radiactivos (ENRESA) as project leader, the French Institut de Radioprotection et de Sûreté Nucléaire (IRSN), the Swiss Nationale Genossenschaft für die Lagerung radioaktiver Abfälle (NAGRA) and the GRS.

Within the project GRS was responsible for the investigation of desaturation and resaturation of the Opalinus clay during the ventilation of a microtunnel simulating the ventilation of a nuclear repository in a geological clay formation.

Detailed information is given about the layout of the measurement array, the measuring instrumentation, and the measurement results obtained between October 2002 and May 2004. Information about laboratory calibration measurements needed for further interpretation of the in situ measuring data is given as well.

The participation of GRS was funded by the German Ministry of Economics and Labour (BMWA) under contract No. 02E9501 and the Commission of the European Communities under contract No. FIKW-CT-2001-00126.

Table of Contents

	Foreword	I
1	Introduction	1
2	Measuring Principles	3
2.1	Measuring Techniques	3
2.2	Measurement Evaluation	4
3	Monitoring System	7
3.1	Hardware Components	8
3.1.1	Resistivity Meter and Embedded PC	9
3.1.2	Electrode Decoder Array	10
3.1.3	Uninterruptible Power Supply	10
3.1.4	Measuring Procedure	10
3.2	Electrodes and Electrode Chains	11
4	Measuring Array Around the Microtunnel	13
5	Laboratory Calibration	15
5.1	Samples	15
5.2	Measurements	17
5.2.1	Density and Porosity	17
5.2.2	Resistivity	18
5.3	Results	20
5.3.1	Density and Porosity	20
5.3.2	Resistivity	21
5.4	Conclusion	23
6	Assessment of Measurement Resolution	25
7	Field Measurements	27
7.1	Geoelectric Tomography Results	27
7.2	Sampling at the End of the Desaturation Phase	32

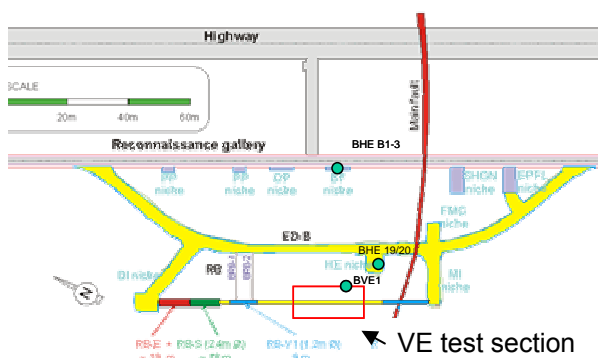
7.2.1	Samples	32
7.2.2	Results	36
8	Summary and Conclusion.....	41
9	Acknowledgements	43
10	References.....	45
	List of Figures	47
	List of Tables	49

1 Introduction

The Ventilation Experiment (VE) experiment was carried out at the Mont Terri underground laboratory.

The main objective of the experiment was to evaluate “in situ” the desaturation of consolidated clay formations in consequence of the ventilation of underground openings of a repository in a geological clay formation.

The test has been arranged in a non-lined horizontal microtunnel of 1.2 m diameter (Figure 1-1). The microtunnel was excavated using the raise-boring technique (but in horizontal) in the Opalinus clay formation. A 10 m long test section was sealed off by means of two double doors and subjected to a de-saturation and saturation cycle by ventilation during a period of about 10 months. The test section was ventilated by a 40 m³/h airflow rate with a variable relative humidity between 20 – 90 % at ambient temperature of about 15 °C.



a) Position of VE test section in the URL

b) View into the microtunnel

Figure 1-1 Microtunnel at the Mt. Terri Underground Research Laboratory (URL)

The test section (the surrounding rock and the microtunnel itself) was monitored by a total of 120 sensors (Figure 1-2) to measure different parameters, such as rock displacement, water potential and water content, temperatures, ventilation air conditions, etc. For that purpose about 85 boreholes were drilled in the rock to monitor its response to the ventilation.

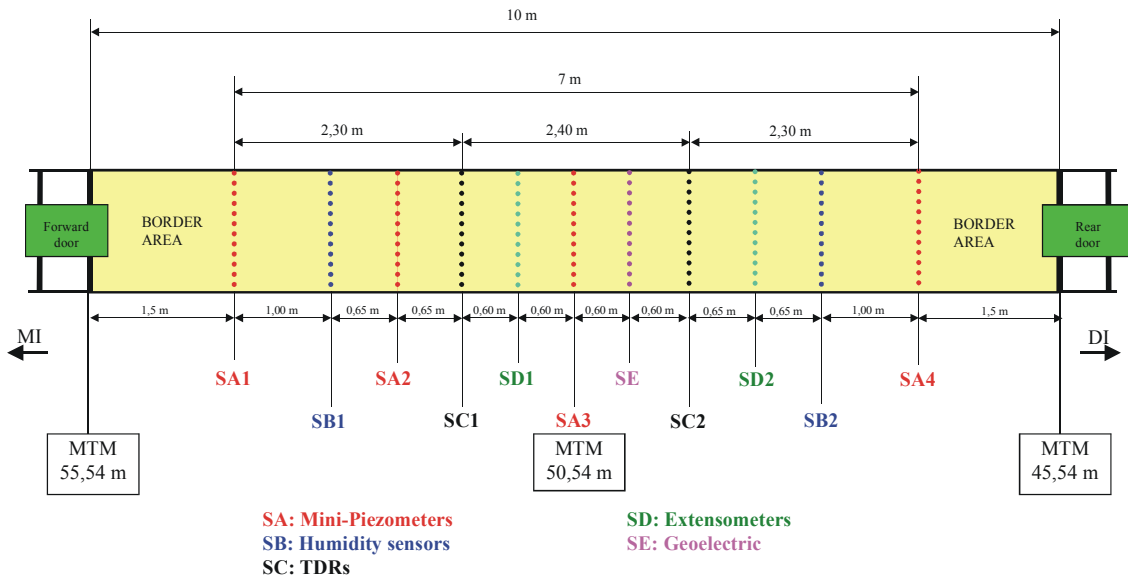


Figure 1-2 Instrumented VE test section in the microtunnel at the Mt. Terri Underground Research Laboratory (URL)

This report describes geoelectric measurements performed by GRS to determine the evolution of the desaturated zone in a quarter section around the microtunnel.

The electric resistivity of the clay rock around the microtunnel was determined by use of a multi-electrode array. The array consists of five electrode chains. The resistivity distribution in the area between the chains was determined by means of tomographic dipole-dipole measurements. The recording unit for these arrays was controlled remotely from Braunschweig/Germany through a telephone connection, which allows periodic measurements of the in-situ resistivity distribution. From the measured apparent resistivity values the "true" resistivity distribution is computed applying the Software package SensInv2D /FEC 01/.

In the geoelectric measurements advantage is taken of the dependence of the electric resistivity of materials on the water (solution) content. In order to interpret the resistivity values in terms of water content the data are to be compared with calibration results which were derived from pre- and post-test laboratory measurements.

2 Measuring Principles

2.1 Measuring Techniques

The technique most frequently applied for geoelectric measurements in the field is the four-point method (Figure 2-1). An electric direct current (DC) is supplied to the formation via two electrodes. The magnitude and direction of the resulting electric field are dependent on the conductivity conditions in the rock. The potential difference between two other electrodes is measured. The input electrodes (C_1 , C_2) and the output electrodes (P_1 , P_2) are arranged as single dipoles (Figure 2-1). For a medium with spatially constant electric resistivity, the resulting potential difference ΔV is given by Ohm's law (equation 2-1), so that the resistivity ρ can be derived from a single measurement.

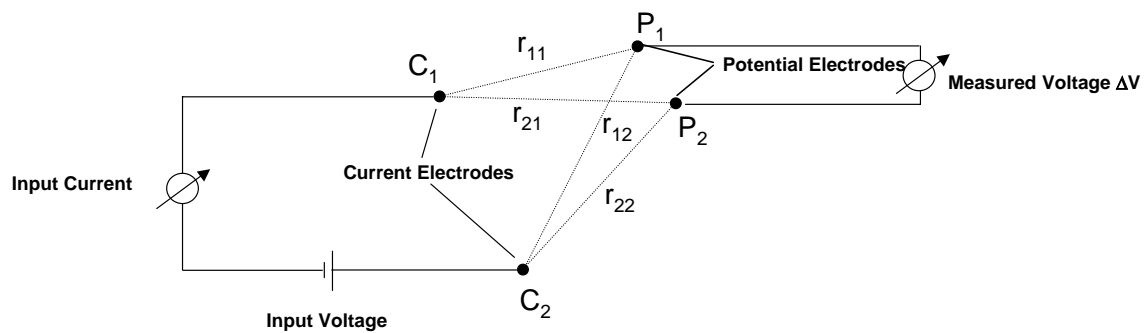


Figure 2-1 Principle configuration of a dipole-dipole measurement

$$\Delta V = \frac{1}{4\pi} I\rho \left(\frac{1}{r_{11}} - \frac{1}{r_{12}} - \frac{1}{r_{21}} + \frac{1}{r_{22}} \right) \quad (2-1)$$

In the normal case of a spatially varying resistivity, the resistivity obtained by evaluating equation 2-1 for a single measurement is an apparent resistivity. A large number of measurements with different current and potential dipoles is required to reconstruct the real resistivity distribution (see next section). For a complete data set, the position of the input dipole is fixed and the output dipole is moved around the area to be investigated. Afterwards, the input dipole is moved to another position, and the measurements are repeated.

Further details on the theoretical principles of DC geoelectrics can be taken from /FLA 01/:

Although methods of DC geoelectrics are employed for the evaluation of the measurements, modern geoelectric systems use low-frequency alternating current (AC) rather than direct current. The reasons are:

- Direct current would cause electrolytic polarization, i. e., concentration of ions around the electrodes. This is prevented by periodic reversal of the current.
- Telluric currents, i. e., natural electric currents in the ground, can be accounted for in the measurements when the current is reversed and the measurement results are averaged, since the telluric currents do not change their polarity.

2.2 Measurement Evaluation

Measurement evaluation is performed by inverse finite element modelling. Starting with a usually homogeneous model, the expected vector of apparent resistivities for the set of measurement configurations is calculated and compared to the actually measured apparent resistivities. The model is then iteratively improved in order to minimize the deviations between calculated and measured values.

The finite element mesh has to be adapted to the electrode array. The maximum attainable resolution is half the electrode spacing; this is the minimum side length of the finite elements. On the other hand, the attainable resolution has to be considered when designing the electrode array. Half the electrode spacing is the theoretically maximum attainable resolution – if an electrode was placed at every second grid point of the mesh, the inversion result would be definite. In reality, such a high number of electrodes and related measurement configurations is not feasible. Consequently, there are areas further away from electrodes where resolution and accuracy decrease. Therefore, scoping calculations are necessary before installing the electrodes in order to find out whether the expected effects can be detected (see Section 6).

For the evaluation of the measurements, GRS uses the commercial software package SensInv2D /FEC 01/ which allows a two-dimensional inversion of the measured apparent resistivity data. Several strategies for applying iterative improvements to the resistivity model are implemented in this software. GRS employs the multiplicative

simultaneous inversion reconstruction technique (MSIRT) /KEM 95/ which is controlled by the sensitivity distribution of the model.

Each single measurement configuration gives a so-called sensitivity distribution, which is the matrix of partial derivatives of measured impedance against resistivity. Thus, the sensitivity at a special finite element describes how sensitive the result of this single measurement is to changes in resistivity. The cumulative sensitivity is the sum of the sensitivity matrices of all single measurements, thus describing where a resistivity change has a high influence on the overall results, and where not. Cumulative sensitivity is a measure for accuracy and reliability of the resistivity results. It is usually highest near the electrodes and lowest farther away.

Evaluation of the geoelectric measurements leads to a two-dimensional resistivity distribution that is supposed to be close to the true resistivity field. In order to interpret this resistivity distribution in terms of water content distribution, laboratory measurements have to be performed at defined saturation conditions (see Section 5). Using the results of the laboratory calibrations, information on water content can be derived from the resistivity distribution.

3 Monitoring System

All geoelectric systems employed by GRS use low-frequency alternating current. Typically, 2 to 5 current cycles are injected during a single measurement. The period of a cycle is usually between 5 and 10 seconds. Such low frequencies are necessary in order to be able to treat the measurements as direct current geoelectrics; higher frequencies may result in phase differences between injected current and measured voltage. The injected current is in the range between 1 and 200 mA.

Originally, the geoelectric system employed in the frame of the Mont Terri HE-B was extended for performing also the measurements in the Ventilation Test. This is an older system based on a SYSCAL resistivity meter and is described in detail in /YAR 89/. Recurring problems with this system made a replacement necessary. From May 2003 on, the commercial RESECS system (Geoserve, Kiel/Germany) was used for the geoelectric measurements.

The RESECS system is a PC-controlled DC-resistivity monitoring system for high resolution tomography and other geoelectric applications. The RESECS measuring program runs under MS-Windows98. Up to 240 electrodes are separately addressable by unique decoder addresses. Any pair of electrodes might be selected as current injector. Up to six other pairs of electrodes might serve as potential electrodes for simultaneous geoelectrical measurements (six channel operation). The software controlled fast switching of electrodes results in a high data acquisition rate - up to a few thousands data points per hour.

Features of the stand-alone system are its flexible usage and its convenience in creating geoelectric standard configurations (Wenner, Schlumberger, Dipole-Dipole etc.) as well as user-defined configurations for multi channel applications. All measuring parameter input is menu-driven.

In measuring mode RESECS automatically selects all programmed electrode configurations. It optimizes preamplification, corrects self potentials and yields DC-resistivity (ρ , U, I) as well as IP-values (phaseshift, chargeability). For standard configurations pseudosections and pseudodepth slices are displayed simultaneously. Current injection and its resulting potential differences are displayed online and can be stored on harddisk for later processing.

3.1 Hardware Components

The whole measurement system essentially consists of the following components:

- Resistivity meter and embedded PC
- Electrode decoder array
- Uninterruptable power supply

The resistivity meter and the embedded PC are integrated in a waterproof and dust-proof compact military standard housing (Figure 3-1). The complete encapsulation of the system was considered necessary because of significant dust development usually occurring during drilling campaigns at Mont Terri Underground Research Laboratory (URL).



Figure 3-1 RESECS measuring system

The seven decoder-array boxes with 16 decoders each are contained in a waterproof and dust-proof military standard housing, too (Figure 3-2).

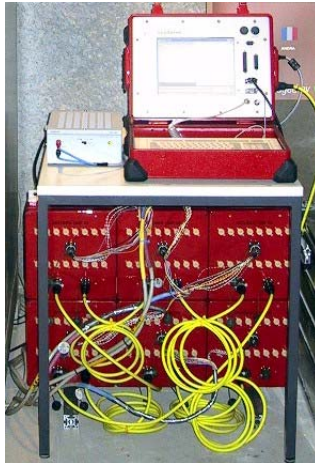


Figure 3-2 Decoder boxes of geoelectric monitoring system

The uninterruptible power supply is not integrated, but was delivered as two stand-alone 19"-plug-in modules, which are mounted in a small 19"-enclosure.

3.1.1 Resistivity Meter and Embedded PC

The resistivity meter is controlled by the embedded PC. Up to six potential differences can be measured simultaneously. Each analog input signal (injection current, potential differences) is supplied with a separate signal path. These signal paths are galvanically isolated from each other and from the embedded PC as well. Each one consists of high quality amplifiers (for impedance adaption, programmable gain setting and isolation), optocouplers and DC/DC converters for the separation of power supplies. Furthermore each signal path is supplied with a DC-accurate, tunable linear phase 5th order Bessel lowpass filter. The cutoff frequencies are software selectable. The AD-converter has a resolution of 16 bit and a conversion interval of 1 ms for each channel.

The injection voltage is switched using a full bridge consisting of high voltage transistors (FET). The switching timing is defined by software.

The electrode address code is created electronically by converting digital PC output to a serial function and address code.

The embedded PC is supplied with 33 MByte DRAM. The PC is set to the requirements of the measuring system. For detailed information refer to the PC510 users manual supplied on disk.

3.1.2 Electrode Decoder Array

Electrode decoders are electronic circuits used for switching relays to the measuring lines C_1 , C_2 , P_1 or P_2 . Each decoder has a unique address and four different functions. Decoders are supplied in groups of 16.

Activating and deactivating of electrode decoders is controlled by the measuring software. All decoders included in a measuring cycle are selected before the measurement and deselected before the next one. Only those decoders used for the next measuring cycle with the same function will not be deselected.

The supply voltage for the decoders is generated within the RESECS system.

It is galvanically isolated from other parts of the system. The decoder and relay supply current is displayed on the ampere-meter on the front of the system.

3.1.3 Uninterruptible Power Supply

The system is supplied with an uninterruptible power supply, Xanto 2kVA. The purpose of the UPS is to provide power to the entire measuring system for at least 180 minutes in the event of voltage breakdown or power failure.

3.1.4 Measuring Procedure

The RESECS measuring software runs under MSWindows98. All input of measuring parameters is menu-driven. The systems offers the possibility to create standard configurations like Wenner, Schlumberger, Dipole-Dipole as well as user defined configurations.

User defined configurations enable multi channel measurements. Up to six potential differences can be recorded simultaneously. These measurements require an user defined ASCII input file.

After creating a standard master project or an user defined master project all measurements can be controlled manually or automatically.

In monitoring mode the software creates copies of the master project and executes these daughter projects automatically. RESECS offers the opportunity to choose between different monitoring modi like start time controlled, interval controlled, number

of cycle controlled or any combination of them. All measured values are stored on harddisk.

In the monitoring mode the voltage across the current electrodes is limited by software to 60 V for security reasons.

3.2 Electrodes and Electrode Chains

To achieve optimum measuring results and to avoid an unnecessary impact on the local resistivity by water containing grouts a special electrode chain design was used at Mt. Terri. An electrode chain consists of a bundle of single electrode cables each of which being soldered to a 5 mm electrode which is fixed in the wall of a plastic half tube (Figure 3-3). The single cables are sealed in the half tube with silicone and guided out of the borehole where they are connected to a plug which itself will be fixed at the microtunnel wall. The electrodes were pressed against the rock by filling the remaining volume of the borehole with rock powder produced during drilling of the boreholes and compacting the rock powder as far as achievable by stamping with a stick. Filling of the borehole and compaction of the rock powder was made in several steps with small portions of material in order to enable proper compaction of the material over the whole borehole length.

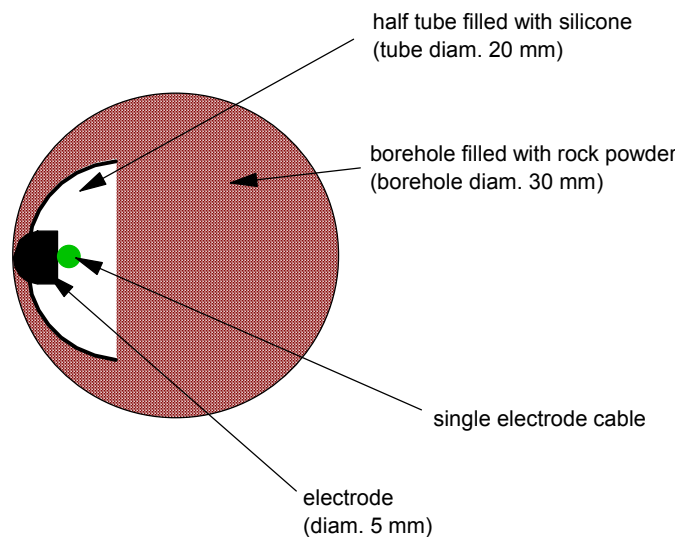
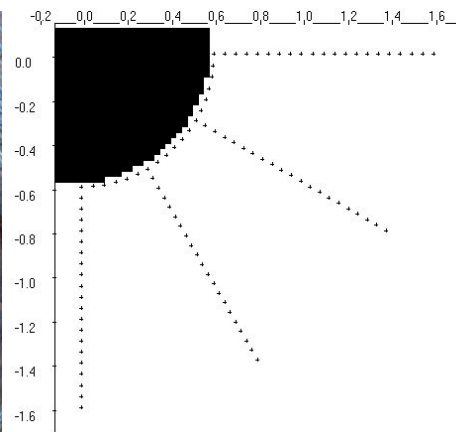


Figure 3-3 Cross section through electrode borehole

4 Measuring Array Around the Microtunnel

The array consists of four electrode chains which are installed in 1 m deep boreholes drilled in a plane perpendicular to the microtunnel axis. The boreholes reach radially away from the microtunnel and are arranged in one quarter section (Figure 4-1). One borehole was drilled horizontally in the microtunnel wall and one borehole drilled vertically down in the microtunnel floor. The two remaining boreholes were drilled equally spaced between the two outer boreholes. The spacing of the electrodes in the boreholes is 5 cm to allow a maximum resolution of resistivity distribution of about 2.5 cm. 80 electrodes were installed in the four boreholes and 19 additional electrodes on the microtunnel wall within the selected quarter section. The complete array thus consists of 99 electrodes.



a) Installation of an electrode chain

b) layout of complete electrode array

Figure 4-1 Geoelectric array around the VE microtunnel

5 Laboratory Calibration

For the interpretation of the geoelectric in-situ measurements to be performed during the Ventilation Experiment (VE) in the Mont Terri URL laboratory calibrations were carried out in the GRS laboratory in Braunschweig in order to determine the relation between electric resistivity and the water content of the Opalinus Clay. The clay samples were investigated at decreasing water content during desaturation by drying in air at ambient conditions and by heating.

5.1 Samples

The investigations were performed on samples BVE 1/1 and BVE 1/2. In the state of delivery, the samples were poured with wax in a plastic tube Figure 5-1. After unpacking, the samples were prepared and investigated without any resaturation at first as reported in /MIH 02/. Subsequently, the resistivities were determined from full saturation down to the dry stage, too. In order to achieve full saturation, the samples were for about 11.5 weeks stored in an exsiccator (Figure 5-2) at 100 % air humidity.



Figure 5-1 BVE sample poured with wax in a plastic tube



Figure 5-2 Exsiccator with clay samples

In Table 5-1 the actual geometrical data and the borehole depths from which the samples were taken are summarized.

Table 5-1 Geometrical data of the investigated samples of the cores BVE 1/1, BVE ½

sample	depth		sample length L	sample diameter d
	m			
BVE 1/1A	6.10	6.22	10.07	7.17
BVE 1/1B	6.22	6.34	10.04	7.16
BVE 1/1C	6.34	6.46	9.97	7.16
BVE 1/2A	7.83	7.95	10.15	7.17
BVE 1/2B	7.71	7.83	10.07	7,18
BVE 1/2C	7.35	7.47	9.96	7.16

5.2 Measurements

5.2.1 Density and Porosity

The porosity Φ of the samples was calculated by the grain density ρ_g and the bulk density ρ_b

$$\Phi = 1 - \frac{\rho_b}{\rho_g}$$

with

Φ porosity, -

ρ_g grain density, kg/m^3

ρ_b bulk density, kg/m^3 .

The grain density was determined at remaining clay material of the BVE samples. The clay was dried at 105 °C and grinded. Afterwards, the grain density of the grinded clay was measured with helium using an air comparison pycnometer after Beckman (Figure 5-3). The bulk density was determined from the dry mass and the volume of the samples. The porosity of each sample was calculated using the bulk density and the grain density of the grinded material.



Figure 5-3 Air comparison pycnometer (after Beckman)

5.2.2 Resistivity

The resistivity of the samples was determined by using the four-point method. Here, the current I is injected at the end surfaces of the sample and the difference in the electrical potential U is measured at the voltage electrodes M and N (Figure 5-4).

The resistivity is then calculated according to [TEL 90]:

$$\rho = \frac{U \cdot A}{I \cdot a}$$

with:

- ρ resistivity, Ωm
- U electrical potential, V
- I current, A
- a distance of the electrodes M and N, m
- A cross section area, m^2

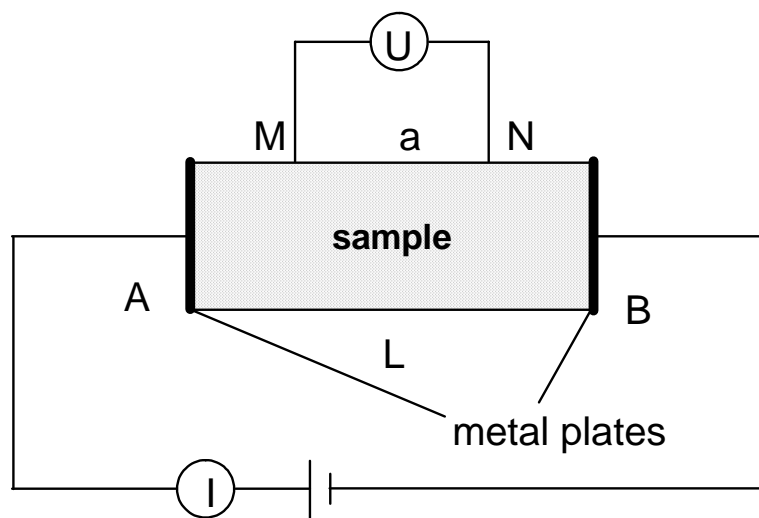


Figure 5-4 Schematic of the 4-point arrangement for the determination of the resistivity

Figure 5-5 shows a photo of the measurement set-up. For a better coupling of the electrodes to the rock samples, the end surfaces were coated with conductive silver lacquer. For the voltage electrodes M and N, two rings of conductive silver lacquer were applied over the circumference of the samples.

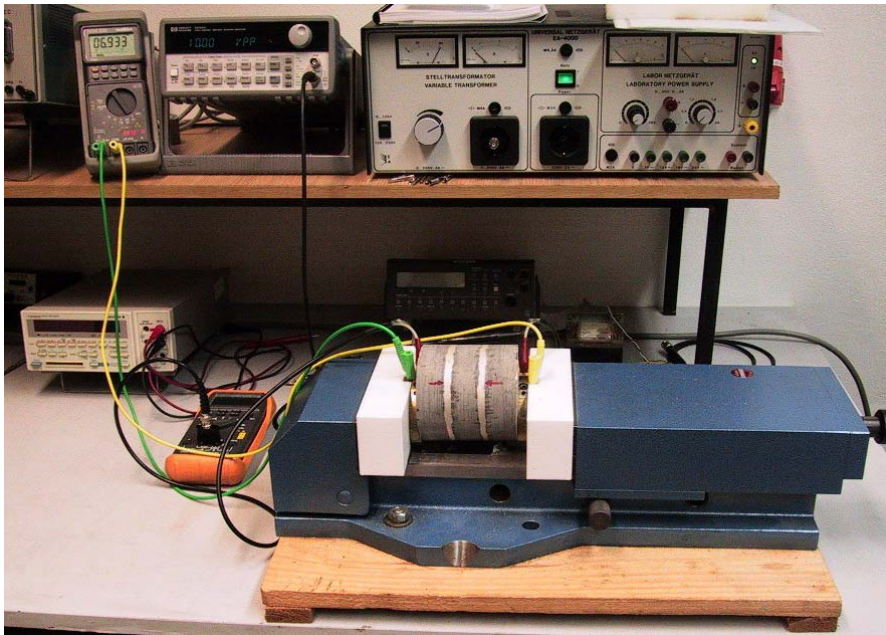


Figure 5-5 Measurement set-up for determination of clay rock resistivity

First, the BVE-samples were investigated at the state of delivery without any additional saturation in order to determine the starting resistivity of a Mt. Terri sample. Resistivities at lower water content were then determined by drying at ambient conditions. Because the BVE-samples were to be investigated subsequently also from full saturation down to the dry stage like the HE-samples, they were not dried at 105 °C in order to prevent any sample damage due to heating.

Afterwards, the samples were saturated. Starting from the state of full saturation, the water content of the samples was reduced at different steps. First by drying at ambient temperature, then under vacuum and later also by heating. At each stage of drying or saturation, the resistivities were measured, respectively. Because the water content w is given by the individual wet mass m_w in relation to the dry mass m_d , the samples were finally dried at 105 °C to constancy of mass which is assumed to represent the completely dry mass. The actual water content was then calculated on basis of the

actual mass reduction during the individual drying steps under consideration of the initial water content and calculated by

$$w = \frac{m_w - m_d}{m_d} = \frac{m_w}{m_d} - 1$$

with:

- w water content, -
- m_w mass of the wet sample, kg
- m_d mass of the dry sample, kg

5.3 Results

5.3.1 Density and Porosity

The grain density of the BVE clay was determined to 2.73 g/cm³. The mean bulk densities of the samples BVE 1/1A to BVE 1/2C ranged from 2.25 g/cm³ to 2.29 g/cm³ (average: 2.27 g/cm³). The resulting porosities were 16.2 % to 17.7 % (average: 17 %). The determined bulk densities and porosities are summarized in Table 5-2.

Table 5-2 Bulk densities, porosities, and water contents of the investigated BVE samples; grain density: 2.73 g/cm³

sample	bulk density (dried at 105 °C)	porosity	water content at state of delivery	water content after saturation
	[g/cm ³]	[%]	[%]	[%]
BVE 1/1A	2.28	16.8	6.31	7.65
BVE 1/1B	2.28	16.5	6.32	7.83
BVE 1/1C	2.25	17.6	6.34	7.86
BVE 1/2A	2.29	16.2	6.35	7.55
BVE 1/2B	2.27	17.0	6.32	7.33
BVE 1/2C	2.25	17.7	6.30	7.27

The grain density reported in /HOH 98/ is about 2.64 g/cm³ (carbonate-rich facies). The bulk densities range between 2.47 g/cm³ to 2.55 g/cm³ (carbonate-rich facies) and 2.37 g/cm³ to 2.33 g/cm³ (shaly facies), respectively. Porosity values from 12.25 % to

17.1 % (shaly facies) were observed. For the measurements, different kinds of preparation were described. The water content of the samples was determined by drying at 105 °C and ranges between 6.6 % and 7.5 % for the shaly facies.

The values in the present report are in good agreement with those described in /HOH 98/. Differences might be explained by different methods of measurements and preparation as well as by different facies.

5.3.2 Resistivity

The resistivities of the samples BVE 1/1 and BVE 1/2 were not significantly different. In the state of delivery (water content approx. 6.3 wt%), the resistivities ranged between 6.3 Ωm and 8.8 Ωm . The drying process at ambient conditions led to a water content of about 3.2 wt% and an increase in resistivity between 18.6 Ωm and 28.2 Ωm . The measured values are plotted in Figure 5-6. The results show that the resistivities increase only slightly up to a water content of about 4.8 wt%, but increase more significantly with progressing dewatering up to a water content of 3.2 wt% where resistivities of 18.5 Ωm to 28.2 Ωm are measured.

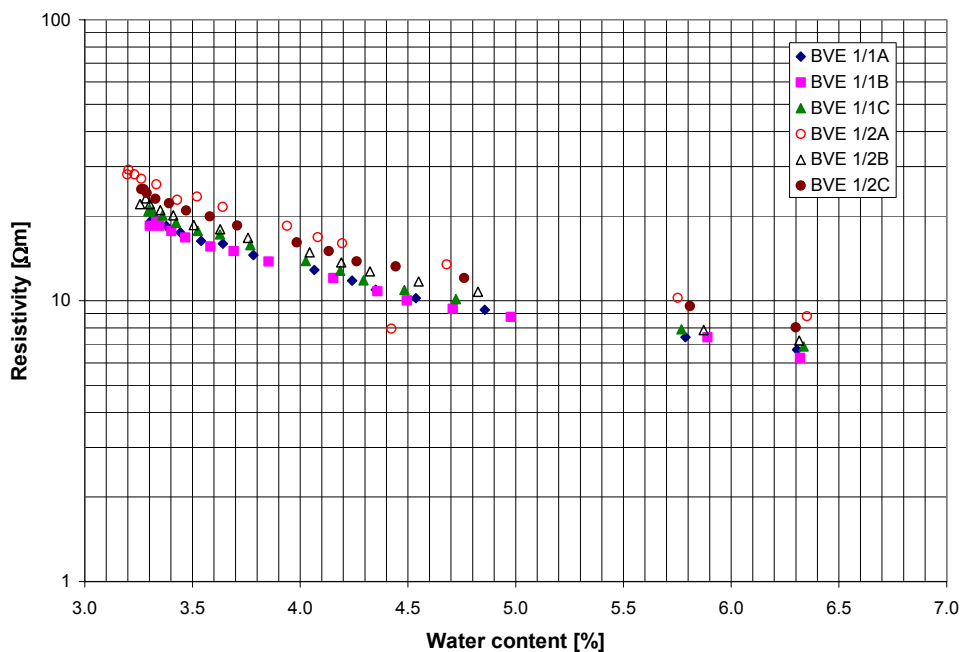


Figure 5-6 Results of the resistivity measurements at the state of delivery without additional saturation

After resaturation, the water content of the samples amounted to 7.3 wt% to 7.8 wt%, and resistivities between $4.7 \Omega\text{m}$ to $7.2 \Omega\text{m}$ were measured. At a water content of approx. 4 wt%, the resistivities with values between $15.3 \Omega\text{m}$ and $26.5 \Omega\text{m}$ were about 3.5 times higher. At a lower water content below 4 wt%, the resistivities increase steeper up to $174 \Omega\text{m}$ and $237 \Omega\text{m}$, respectively. The corresponding water content was approx. 1.4 wt%. The results are plotted in Figure 5-7. In general, this figure shows that the resistivities of the investigated samples were in good agreement.

The combination of both measurements is shown in Figure 5-8. In spite of the different procedures, the results are quite comparable. Obviously, the saturation had no influence on the behaviour of the samples. The measurements at comparable water contents are repeatable. The water contents of the samples at state of delivery and after saturation are also shown in Table 5-1.

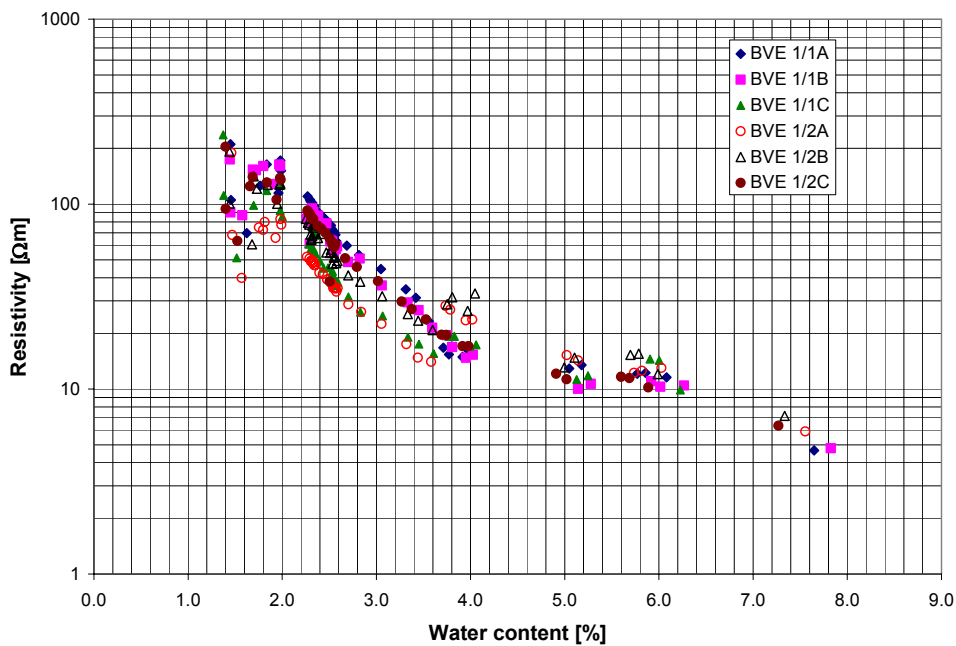


Figure 5-7 Results of the resistivity measurements after saturation and drying

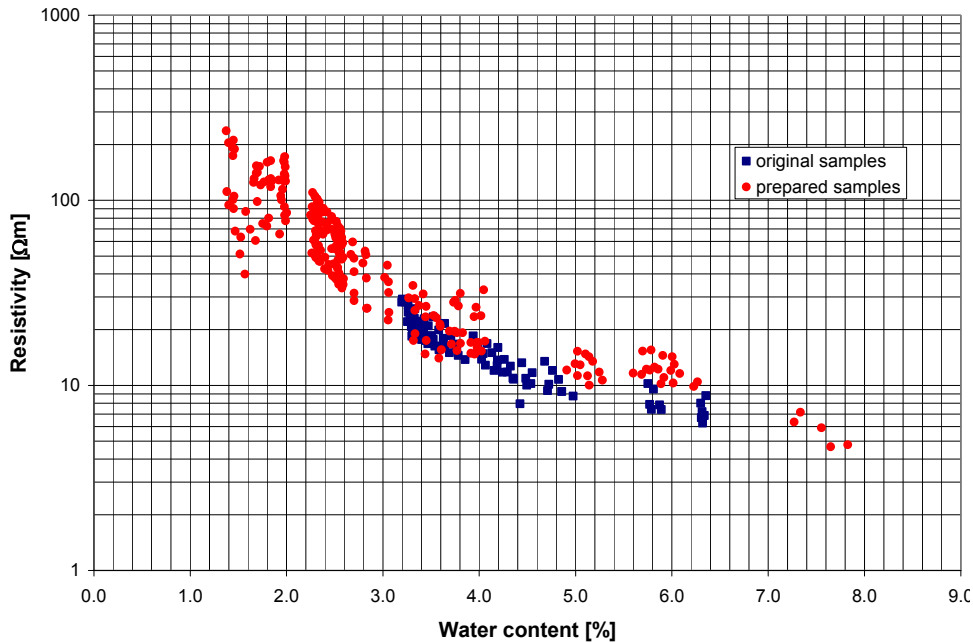


Figure 5-8 Combination of the results of the resistivity measurements after saturation and drying, and at the state of delivery without additional saturation

5.4 Conclusion

The investigations of the BVE-samples were performed in two different ways. In a first step, the samples were investigated in the state of delivery at a water content of about 6.3 wt% without initial resaturation. For these first investigations, the samples were dried at ambient temperature conditions down to a water content of approx. 3 wt%. The resistivities at each drying step were determined ranging between 6.3 Ωm up to 28.2 Ωm. The most significant increase of resistivity was observed between water contents of 4.8 wt% up to 3.3 wt%.

In a second step, the samples were first saturated in an exsiccator at 100 % air humidity. The resistivity measurements were then started at the state of full saturation which corresponds to a water content of about 7.3 wt% and 7.8 wt%, respectively. The different water contents were realized by drying at both ambient conditions and later by heating. The resistivity was determined at different states of dewatering. The resistivity ranges between 4.7 Ωm and 7.2 Ωm in the saturated state up to approx. 174 Ωm and

237 Ωm in the dry stage. The comparison of both measurements shows a good agreement of the results.

The investigations showed that the resistivity increases significantly only at higher grades of dewatering.

6 Assessment of Measurement Resolution

In order to see whether the expected saturation changes can be detected with the chosen electrode array and measurement configurations, scoping calculations were performed using various resistivity models as input. Three models were investigated:

- A homogeneous model with a resistivity of 15 Ωm , representing the fully saturated rock,
- a model with an additional 10 cm-wide ring around the tunnel having an increased resistivity of 45 Ωm (corresponding to a saturation of 80 to 85 %),
- a model with a resistivity decreasing continuously from 60 Ωm (70 to 75 % saturation) on the tunnel surface to 15 Ωm at 1 m in the rock.

The results of the laboratory calibration measurements were not yet available when the scoping calculations were performed. Therefore, the assumed relation between resistivity and saturation deviates from the calibration results. This is however, not critical for the interpretation of the scoping calculations.

The procedure was to calculate the expected measurement values (in total 3542 single measurements) for each model and then perform the inversion algorithm on the synthetic measurement data. The homogeneous model was reproduced perfectly. The following figures show the input model and the inversion results for the other two models, respectively. Clearly, both input models are quite well reproduced by the inversion results. Boundary effects, as in the lower right corners of Figure 6-1 and 6-2, do not disturb the results within the electrode array. The method and the chosen electrode configuration were thus expected to be adequate for investigating changes in moisture content during the ventilation test.

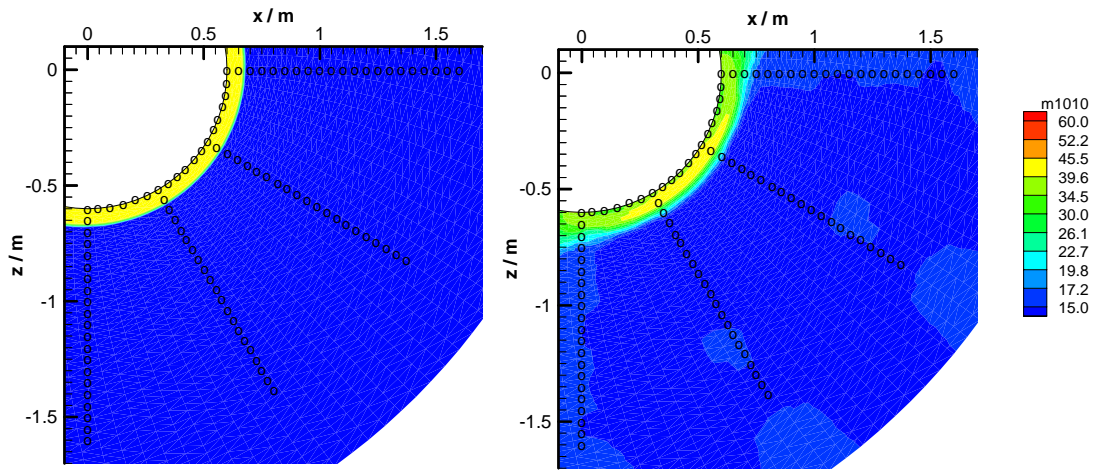


Figure 6-1 Geoelectric modelling of a resistivity distribution with a discontinuous desaturated ring of 10 cm width. Left: Input model, right: Inversion result

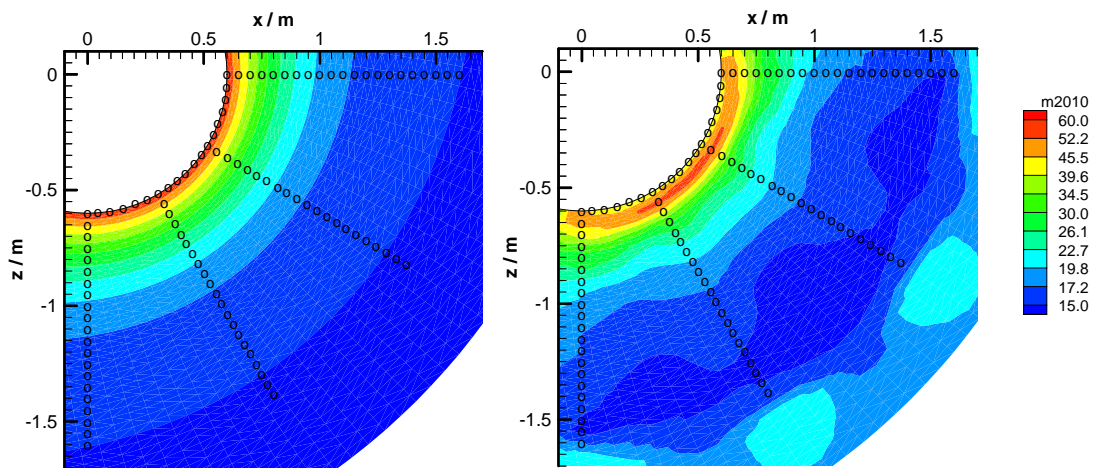


Figure 6-2 Geoelectric modelling of a resistivity distribution with a continuous desaturated zone around the microtunnel. Left: Input model, right: Inversion result

7 Field Measurements

Geoelectric measurements were started in September 2002. From mid October 2002 until mid January 2003, no measurements were taken due to problems with the measuring system. In May 2003, the originally used SYSCAL system was replaced by a RESECS system (see Section 3).

In the following sections, the geoelectric tomography results are presented (7.1) and compared to the results of laboratory investigations on samples taken at the end of the desaturation phase (7.2).

7.1 Geoelectric Tomography Results

The tomograms obtained until April 30, 2003 (Figure 7-1) are rather smooth, with a high resistivity anomaly near the middle of the 30°-electrode chain (red in the figures) and a low resistivity anomaly near the chain ends (blue). The high resistivity anomaly is an artefact caused by an electrode which is not well coupled to the rock. The low resistivity is an artefact as well, caused by the low accuracy of the inversion near the model edge. This becomes obvious when comparing the tomogram of September 2002 (upper left of Figure 7-1) to the following ones. In the first figure, the low resistivity area is much wider. In 2002, a lower injection voltage and thus lower injection currents were used. In 2003, a different voltage supply with higher injection currents was installed in order to improve accuracy of the measurements. As a consequence, the low resistivity artefact diminished.

The remaining areas of the tomograms (Figures 7-1) show a smooth and reproducible resistivity distribution of 6 to 25 Ωm which can be related to almost fully saturated clay rock. The nailed electrodes on the microtunnel surface are better connected to the rock than those in the boreholes. At the tunnel surface resistivities around 6 Ωm prevail, indicating full rock saturation (see Figure 5-8).

From May 2003 on, coupling of several of the electrodes, especially in the lower portions of the vertical and inclined boreholes, became gradually worse, which disturbed the resistivity results of the whole model. The reason is not clear; it could be a corrosion effect. In order to get around this problem the model was reduced and only those borehole electrodes located in the near-tunnel half of the boreholes were

considered for evaluation. The lower right tomogram of Figure 7-1 shows the results obtained with the reduced model for the measurement of April 30, 2003.

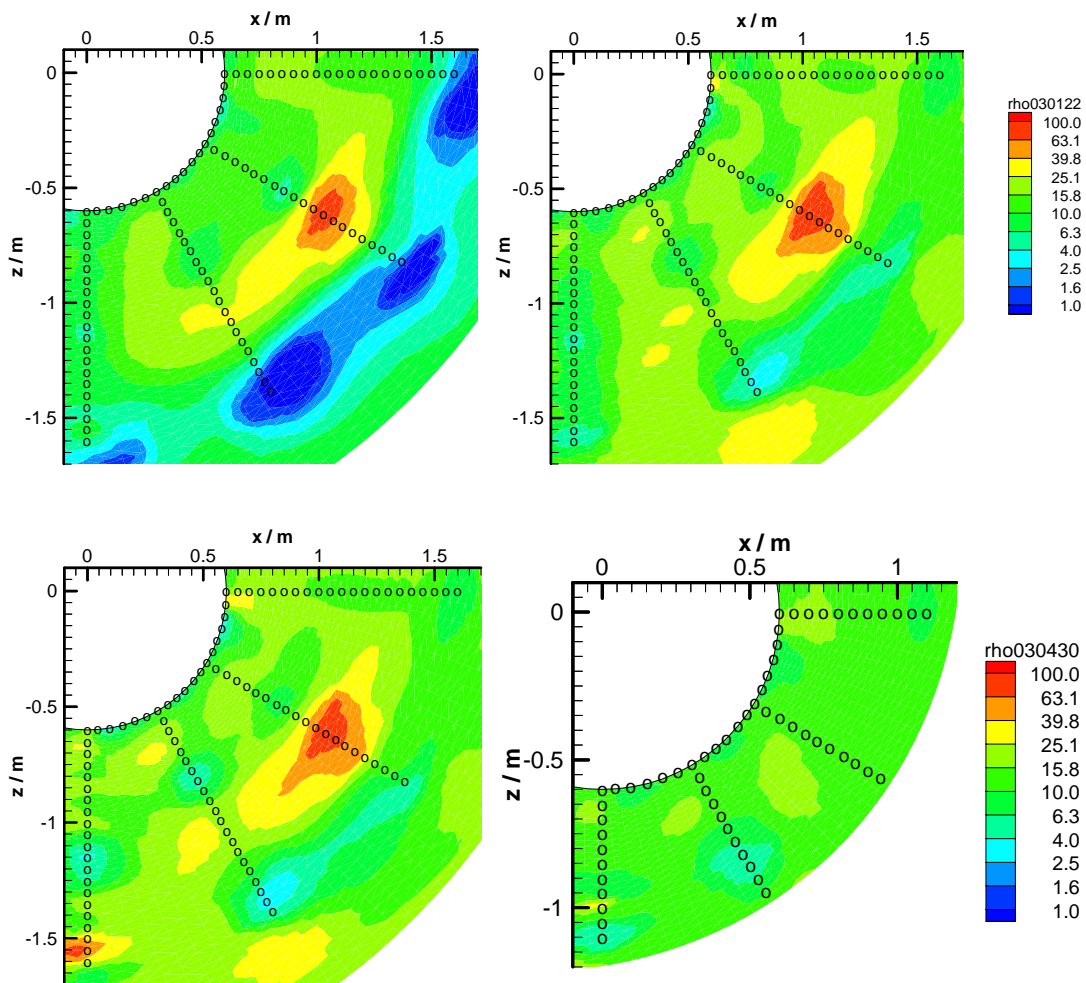


Figure 7-1 Resistivity tomograms of the first resaturation phase – September 21, 2002 (upper left), January 22, 2003 (upper right), April 30, 2003 (lower left), and the reduced tomogram of April 30, 2003 (lower right)

In the beginning of July 2003, ventilation with 30 % of humidity followed the resaturation phase. Since September 4, 2003 the microtunnel was ventilated with 0 to 20 % air humidity. The tomograms of this desaturation phase are shown in Figure 7-2. Until January 25, 2004 (lower right of Figure 7-2) the desaturation effect can be detected in the tomograms as a gradual resistivity increase in a zone of 40 to 50 cm width around the microtunnel. Saturation decreased to about 50 % in the vicinity of the microtunnel until this date (compare Figure 5-8).

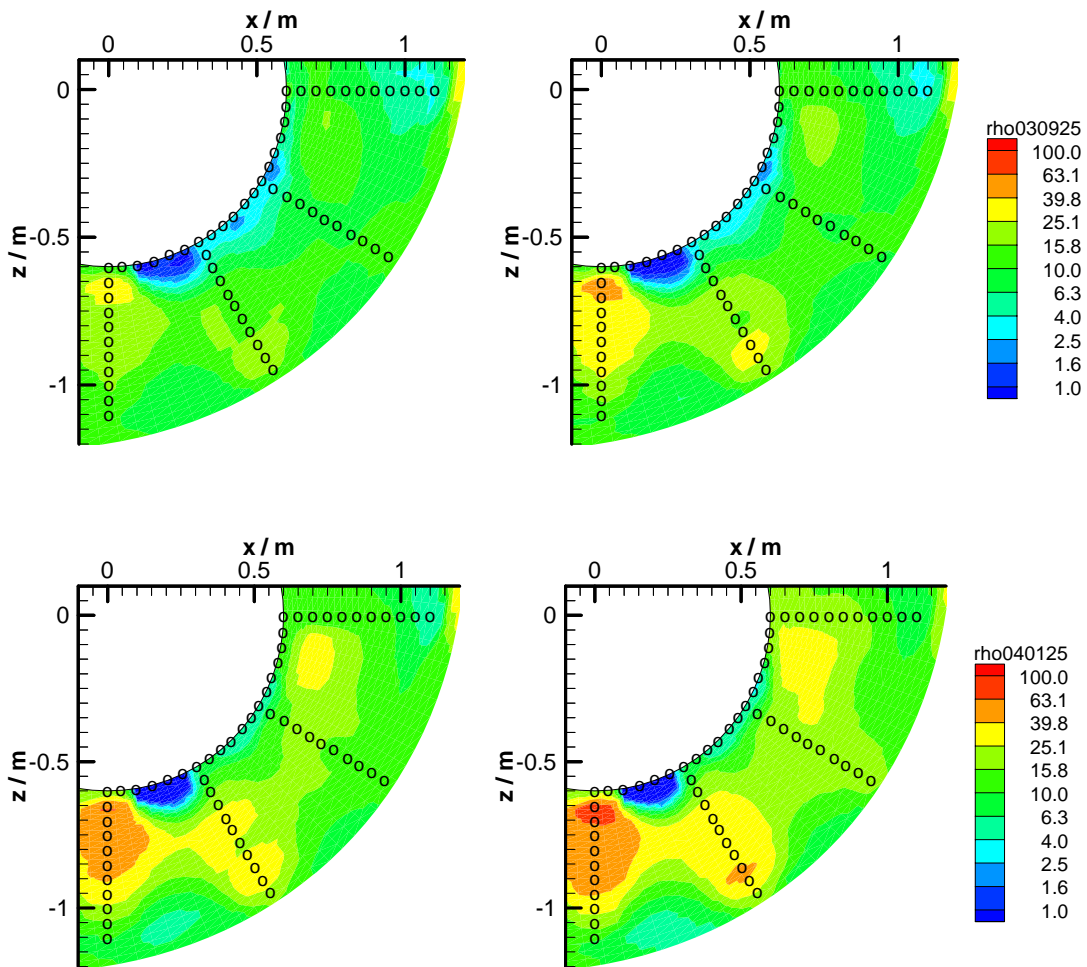


Figure 7-2 Resistivity tomograms of the desaturation phase – August 21, 2003 (upper left), September 25, 2003 (upper right), November 16, 2003 (lower left), and January 25, 2004 (lower right)

The desaturation effect and the extent of the desaturated zone becomes more visible when the relative change of the resistivity rather than the resistivity itself is plotted in the tomograms. This has been done in Figure 7-3 where the resistivity distributions of September 2003, November 2003, and January 2004 are divided by the respective resistivity distribution of August 2003. The gradual development of a desaturated zone of 40 to 50 cm width is clearly visible.

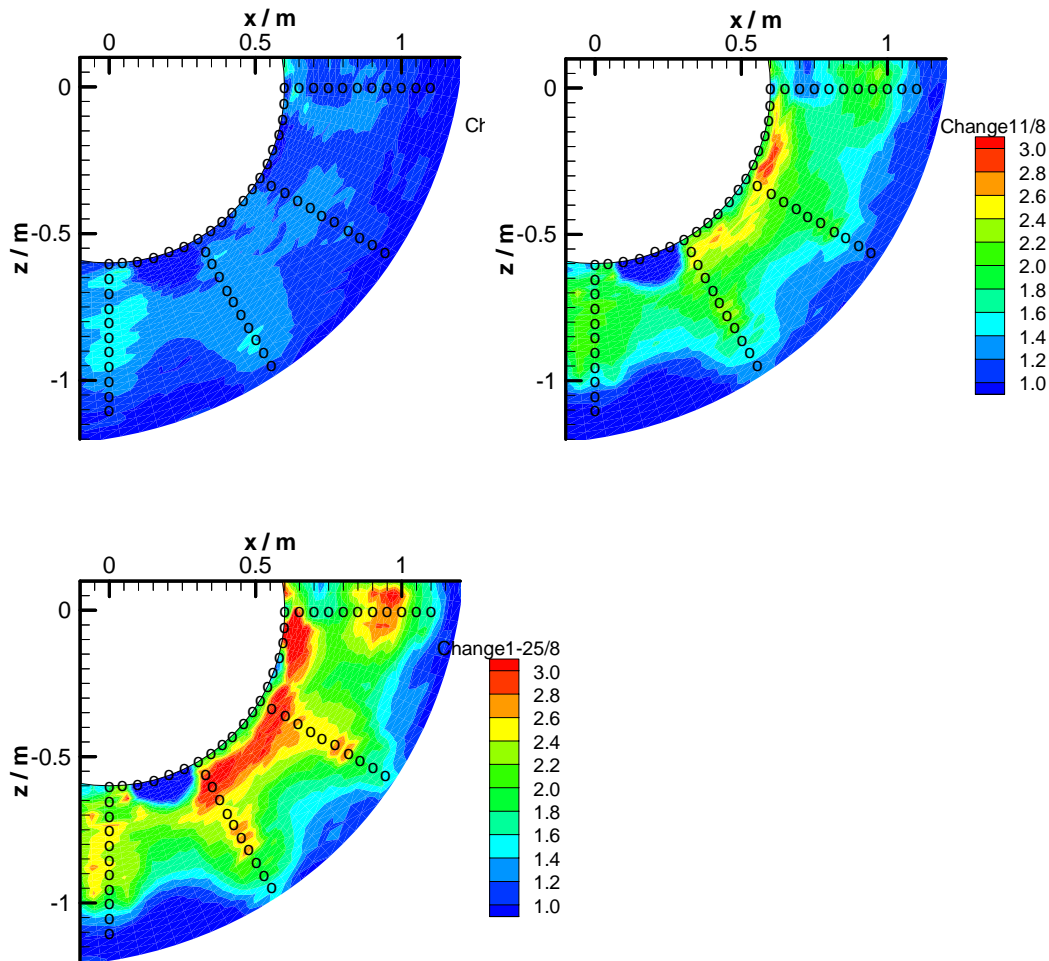


Figure 7-3 Relative change of resistivity during the desaturation phase with respect to the resistivity distribution on August 21, 2003 - September 25, 2003 (upper left), November 16, 2003 (upper right), and January 25, 2004 (lower left). Dark blue = no change, red = increase by a factor of 3

At the end of January 2004, a resaturation phase followed the previous phase. Tomograms obtained during this phase are shown in Figure 7-4. Already on January 31 (upper left of Figure 7-4), a thin saturated zone around the tunnel can be observed. The following tomograms show not only the saturation of this zone near the tunnel, but also a further resistivity increase away from the tunnel, which would mean a further desaturation. It is not yet quite clear how these data have to be interpreted – by a further decrease of coupling quality, or maybe by mechanical alteration of the clay rock as a consequence of the desaturation/resaturation cycle, or by other effects. Interpretation of the measurement results obtained between March and June is made more difficult by the fact that technical problems with the ventilation system led to varying air humidity – higher or lower humidity or natural humidity resulting from

stoppage of the system. A further problem has been a flooding of the microtunnel floor that occurred on April 13, 2004 and led in the succeeding period to desiccation fractures, as reported by AITEMIN /REY 04/. It is possible that the higher contrasts in resistivity, especially the high resistivity values below the floor after that date, are a consequence of this event.

A longer resaturation phase with defined air humidity is needed to obtain clear results.

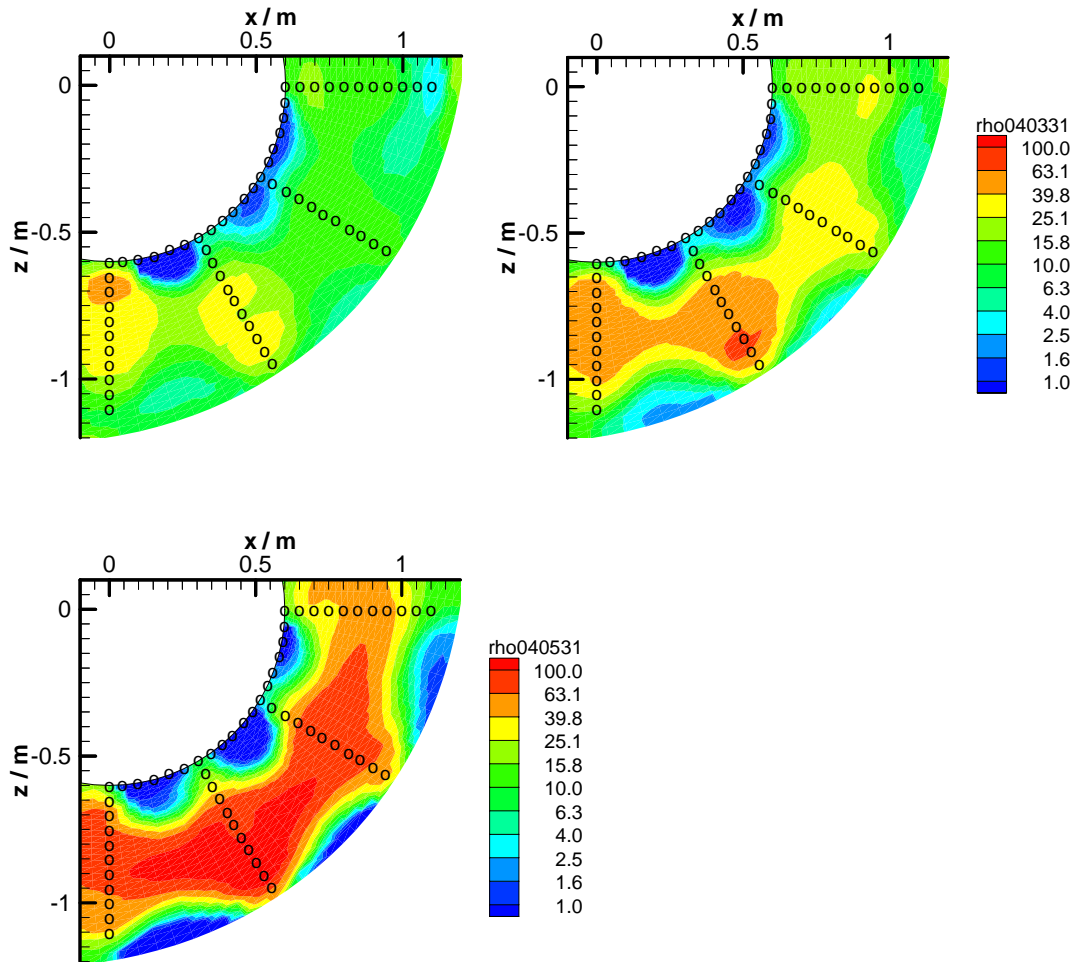


Figure 7-4 Resistivity tomograms of the second resaturation phase – January 31, 2004 (upper left), March 31, 2004 (upper right), and May 31, 2004 (lower left)

Figure 7-5 shows the resistivity evolution at three points in the wall of the micro-tunnel. The gradual resistivity increase during the desaturation phase and the immediate resistivity drop with the start of resaturation are again well represented in this figure.

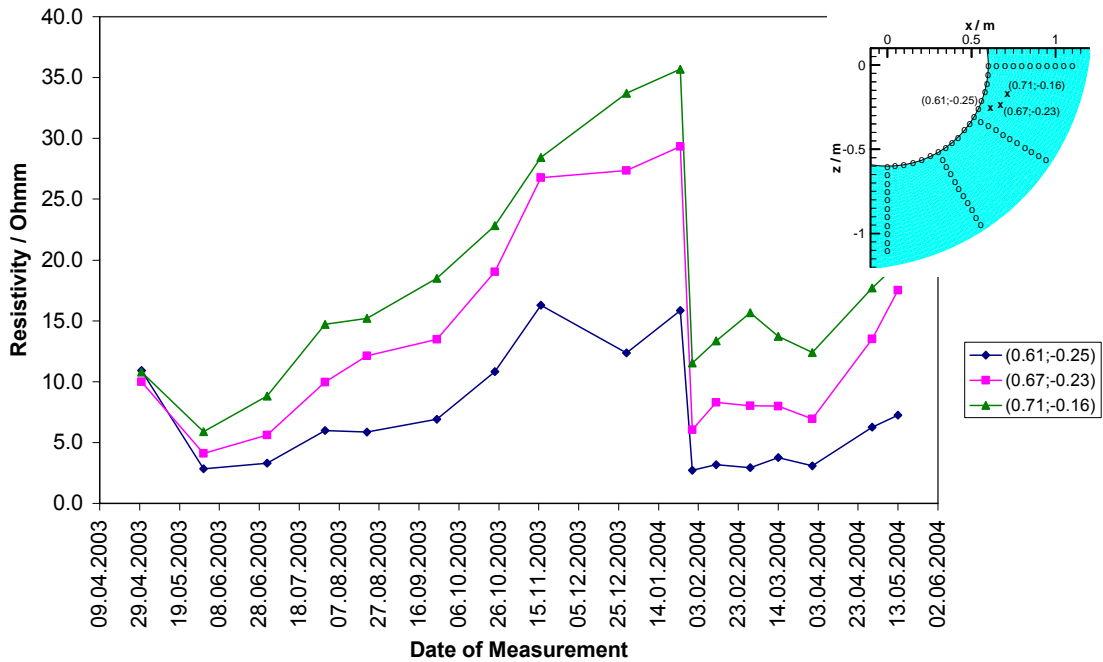


Figure 7-5 Resistivity evolution at three points in the wall of the micro-tunnel

7.2 Sampling at the End of the Desaturation Phase

In order to check and assess the results of the geoelectric in-situ measurements, laboratory investigations on core samples taken after the desaturation phase were carried out at GRS' geotechnical laboratory in Braunschweig. The results of the resistivity measurements were compared with the samples BVE 1/1 and BVE 1/2 investigated before ventilation.

7.2.1 Samples

Three boreholes of 80 cm depth and a diameter of about 6.5 to 6.7 cm were drilled at a cross section located 50 cm distant from the geoelectric cross section SE and 10 cm distant from the TDR cross section SC2 (Figure 7-6). One borehole was drilled horizontally (90°; BVE 87), one with a dip of 135° (BVE 88) and the third vertically into the floor (180°; BVE 89). The arrangement of the boreholes and the positions of the obtained samples are presented in Figure 7-7. The drilling activities took place in the week 5 of 2004 (January 26 to 30, 2004). Immediately after drilling, the samples were wrapped into a metallic coated plastic foil by vacuum.

It was intended to investigate three samples from each borehole. From each borehole, one sample was planned to be taken close to the wall, one from the medium depth (~40 cm) and one from the bottom of the borehole.

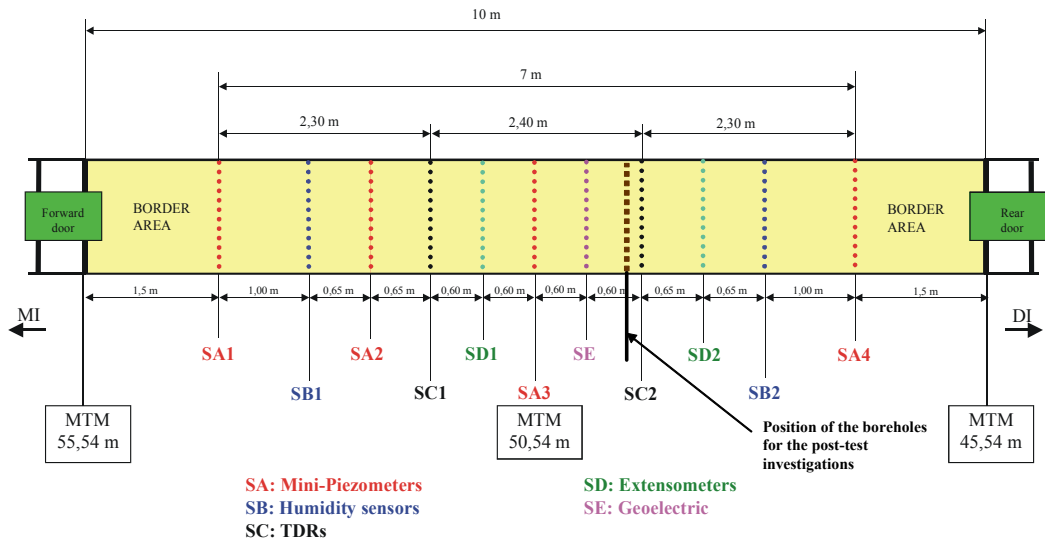


Figure 7-6 Position of the boreholes for the post-test investigations /VE 02/

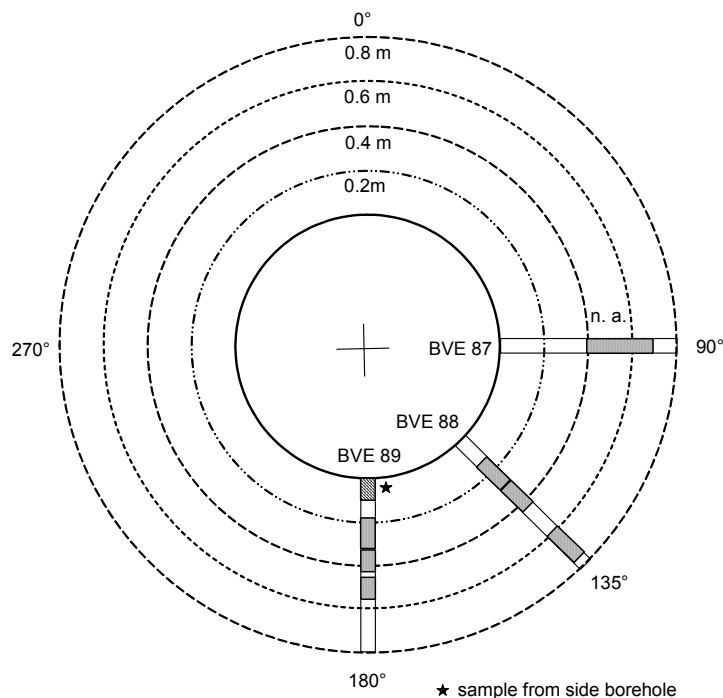


Figure 7-7 Arrangement of the boreholes and position of the samples (n. a.: not available, sample was disturbed)

In order to obtain samples close to the wall, a second side borehole was drilled near the first deep borehole. Only from the boreholes BVE 88 and BVE 89, it was possible to

take some usable core samples. One sample close to the wall was taken from the side borehole of BVE 89. The samples taken from the borehole BVE 87 were too small for laboratory analysis or they were disturbed.

The actual geometrical data and the borehole depths of the obtained samples are summarized in Table 7-1.

Table 7-1 Geometrical data of the investigated samples of the boreholes BVE 88 and BVE 89; (BVE 89 (2.) I was taken from the side borehole)

sample	depth		sample length L	sample diameter d
	cm			
	from	to		
BVE 89 (2.) I	0.5	8.5	8	7.84
be 89 II	21	30.5	9.5	6.51
be 89 III	34	40	6	6.67
be 89 IV	44	53	9	6.67
be 88 V	18.5	28.5	10	6.55
be 88 VI	30	40	10	6.63
be 88 VII	60.5	72	11.5	6.55

Figure 7-8 gives an impression of the arrangement of boreholes with the accompanying side boreholes. Figure 7-9 shows a borehole with a core sample before removal and Figure 7-10 shows two samples taken from the inclined borehole BVE 88.



Figure 7-8 Borehole BVE 87 (above) and BVE 88 (below) with side boreholes



Figure 7-9 View into a borehole before removal of the core sample



Figure 7-10 Two core samples taken from the inclined borehole BVE 88 (depth: 0.15 m - 0.3 m and 0.3 m - 0.44 m)

7.2.2 Results

The results of the measurements are summarized in Table 7-1. For comparison, the resistivities of samples taken from the boreholes BVE 1/1 and BVE 1/2 before starting the ventilation experiment (see Section 5) are included.

Except BVE 89 (2.) I obtained from the side borehole, the water contents of the samples investigated before ventilation as well as after ventilation are not significantly different (see Table 7-2). On the other hand, the resistivities of the samples taken after ventilation are clearly higher than those measured before ventilation (Figure 7-11) and the resistivity data agree quite well with the in-situ measurement data, both qualitatively (with the samples from the vertical borehole having significantly higher resistivities than those from the inclined borehole) and quantitatively (the differences between lab data and tomography results are below a factor 2 for all samples), as can be taken from Figure 7-2.

Table 7-2 Resistivities of Mont Terri VE-samples before and after ventilation;
grain density: 2.73 g/cm³

sample	bulk density [g/cm ³]	porosity [%]	water content [wt.%]	resistivity [Ωm]
before ventilation				
BVE 1/1A	2.28	16.8	6.31	6.69
BVE 1/1B	2.28	16.5	6.32	6.26
BVE 1/1C	2.25	17.6	6.34	6.87
BVE 1/2A	2.29	16.2	6.35	8.81
BVE 1/2B	2.27	17.0	6.32	7.21
BVE 1/2C	2.25	17.7	6.3	8.03
after ventilation				
BVE 89 (2.) I; vertical	2.32	15.3	5.2	35.17
BVE 89 II; vertical	2.34	14.3	6.34	25.96
BVE 89 III; vertical	2.25	17.8	6.5	16.79
BVE 89 IV; vertical	2.21	19.0	6.91	20.22
BVE 88 V; inclined	2.25	17.7	6.35	12.45
BVE 88 VI; inclined	2.30	16.0	6.52	13.37
BVE 88 VII; inclined	2.32	15.0	6.78	12.1

BVE 89 (2.) I: sample from side borehole

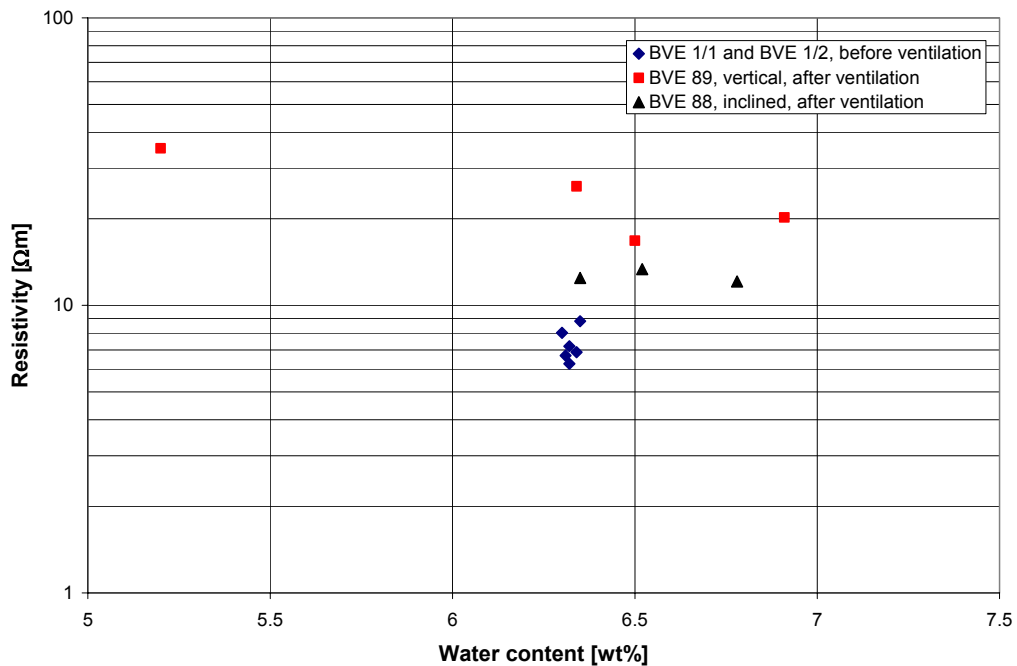


Figure 7-11 Resistivity measurement results of samples obtained before and after ventilation

The resistivities of the samples of the vertical borehole BVE 89 decreased with increasing depth (Figure 7-12 and Figure 7-13). The resistivities are in a range of 16.8 to 35.2 Ωm . The high resistivity of the sample taken close to the wall can be explained by a lower water content caused by the ventilation. In borehole BVE 88 a dependence of the resistivity on depth was not observed. The resistivities ranged between 12.1 and 13.4 Ωm .

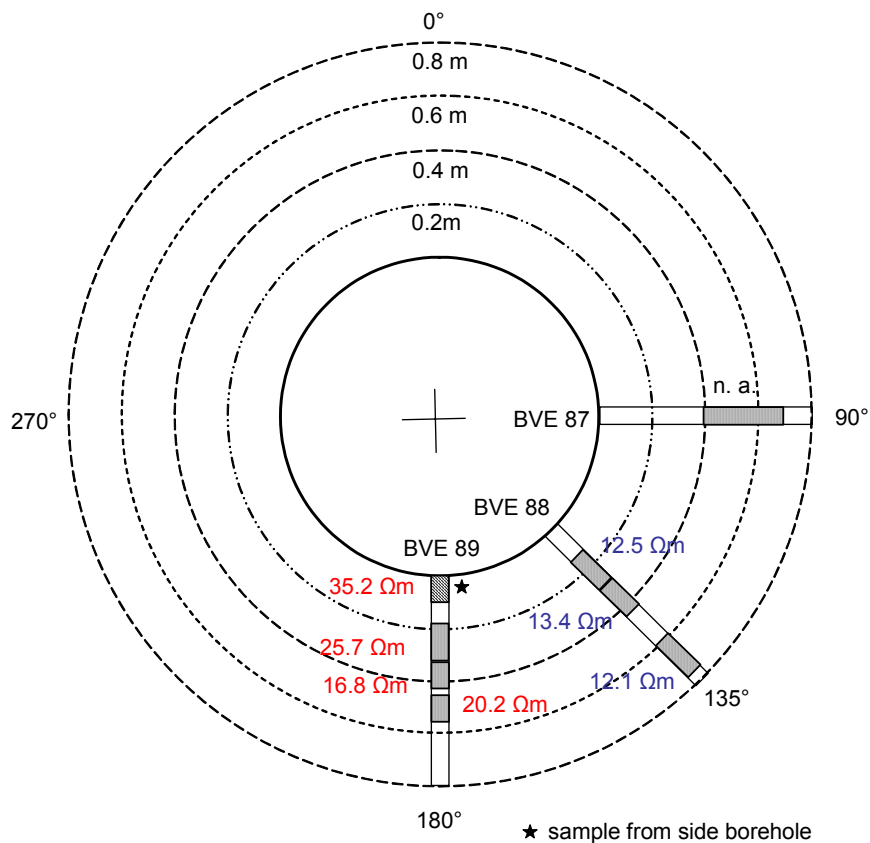


Figure 7-12 Distribution of the resistivities at the depth from which the samples were taken (n. a.: not available)

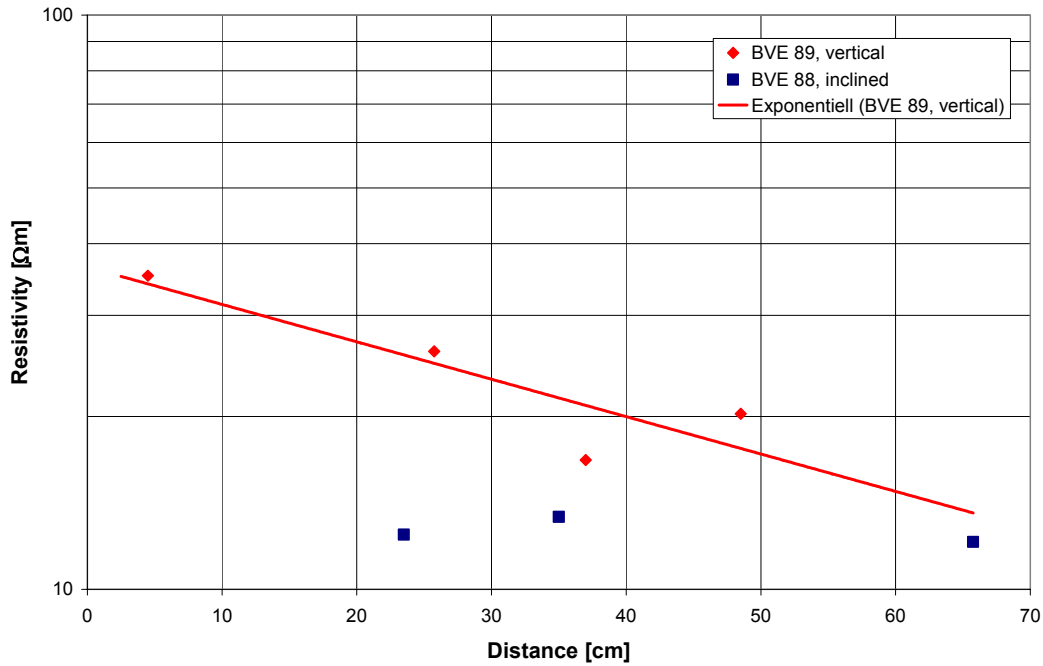


Figure 7-13 Resistivity of the samples taken after ventilation in dependence of the distance from the borehole wall

The discrepancy between the results of the resistivity measurements and the determination of the water content, which showed nearly no significant drying, maybe a consequence of the procedure of water content determination.

Water content of a sample is measured by drying it until weight constancy is reached. This does not necessarily mean that the sample is completely desaturated. Especially for intact clay rock, as investigated prior to the Ventilation Experiment, a residual amount of water is most likely to remain in the sample.

Ventilation obviously led to a deconsolidation and change in the texture, which may have the effect that, in comparison to an intact sample, more water can be released from the sample. If this explanation holds, then ventilation would have led to desaturation, but the water content determination of the samples before and after ventilation would not be comparable.

On the other hand, said change in texture may also have a direct impact on resistivity, so that the results of the resistivity measurements could represent a combined effect of desaturation and deconsolidation.

8 Summary and Conclusion

From December 2001 until May 2004 a ventilation experiment (VE) was performed at the Mt. Terri URL by an international consortium coordinated by ENRESA. Here, a microtunnel of 1.2 m diameter was closed off and ventilated with air of varying humidity in order to monitor desaturation/resaturation in clay rock. After a first saturation phase with humid air a desaturation phase started in July 2003 with a ventilation rate of 30 m³/h and 30 % air humidity. In September, air humidity was set to 0-20 %. The desaturation phase ended in January 2004, since then, the clay rock was resaturated by ventilating the microtunnel with humid air.

In order to monitor the expected changes in water content, four chains of 20 electrodes with a spacing of 5 cm each were installed in boreholes in an array forming a quarter section around the microtunnel. The electrodes were mounted on plastic rods and inserted into the boreholes; afterwards, the remaining space in the boreholes was filled with clay powder and stamped to couple the electrodes to the rock. A fifth electrode chain connects the borehole chains on the tunnel surface.

To enable interpretation of measured resistivity in terms of water content, laboratory calibration tests were performed, which resulted a resistivity of 6 Ωm in the saturated state and up to about 200 Ωm in the dry stage. Model calculations using these results indicated that the geoelectric in-situ measurements should be able to resolve the expected changes in water content induced by the tunnel ventilation in the VE experiment.

Until August 2003, the geoelectric tomograms showed a mostly smooth resistivity distribution of 6 to 15 Ωm which can be related to almost fully saturated clay rock, with small higher resistivity anomalies in the floor. The nailed electrodes on the microtunnel surface are better connected to the rock than those in the boreholes, resulting in low resistivity values near the tunnel surface.

From September 2003 on, the microtunnel was ventilated with 0 to 20 % air humidity. In this phase, a considerable resistivity increase caused by desaturation was observed. At the end of the desaturation phase, a band of 40 to 50 cm width with an increased resistivity had evolved. This becomes more obvious when the relative change in

resistivity as the quotient of the respective resistivity values is plotted. The resistivity increase corresponds to a saturation decrease to a value of about 50 %.

The in situ measuring results indicating drying out effects up to a maximum depth of about 50 cm around the microtunnel were also pretty well confirmed by post-ventilation laboratory investigations performed on cores drilled shortly before termination of the ventilation phase in late January 2004. The results show the increase of resistivity in the direction of the tunnel surface thus confirming the aforementioned conclusions.

An issue occurring during the geoelectric measurements was the worsening coupling of the borehole electrodes to the rock. Here, an improvement is considered worthwhile.

In conclusion, however, it is to be stated that periodic geoelectric measurements were found well suited to determine de- and resaturation in space and time in the consolidated Opalinus clay. Accordingly, geoelectric monitoring will also be performed in the second VE phase intended to be started within the framework of the EU Integrated Project NF-PRO /NFP 03/ in spring 2005.

9 Acknowledgements

The work described in this report was funded by the Projektträger für Wassertechnologie und Entsorgung (PtWT+E) under contract No. 02E9501 and co-funded by the European Commission under contract No. FiKW-CT-2001-00126. The authors would like to thank for this support. Special thanks also to all project partners for their continuous support and the fruitful discussions in the many project meetings.

10 References

- /FEC 01/ Fechner, T. (2001) SensInv2D-Manual, Geotomographie, Neuwied.
- /FLA/ 01/ Flach, D. "Bestimmung der Sättigungsverteilung mittels geoelektrischer Messungen" in Kull, H.; Flach, D.; Graefe, V. (2001): Untersuchung physikalischer Prozesse und Parameter zum Fluid- und Gastransport im Nahbereich von Endlagern in einer homogenen granitischen Gesteinsmatrix, Abschlussbericht zum gleichnamigen Forschungsprojekt des BMFT, FKZ 02 E 8151 A8, Gesellschaft für Anlagen- und Reaktorsicherheit mbH, GRS-172.
- /HOH 98/ Hohner, M.; Bossart, P. (1998): Mont Terri Project: Geological, geochemical, geomechanical and hydraulic parameters of Opalinus Clay derived by in-situ and laboratory experiments (Phase 1, 2 and partly 3).- Technical Note 98-49, April 1998.
- /MIH 02/ Miehe, R., Rothfuchs, T. (2002): Ventilation Experiment (VE) in the Mt. Terri Underground Research Laboratory. - Interim Report on laboratory calibration measurements on clay samples from VE-test field for the determination of the resistivity of the Opalinus Clay at different water content, Deliverable D7b, EC Contract FIKW-CT2001-00126
- /NFP 03/ SCK/CEN, 2003; "NF-PRO: Understanding and physical and numerical modelling of the key processes in the near-field, and their coupling, for different host rocks and repository strategies", Description of Work, EU Contract No.: FI6W-CT-2003-02389
- /REY 04/ Rey, M., Sanz, F. J., García-Siñeriz, J. L. (2004): Ventilation Experiment Status Report 03 – Activities carried out during week 25 (year 2004), AITEMIN, unpublished.
- /TEL 90/ Telford, E. M.; Geldart, L. P.; Sheriff, R. E. (1990): Applied Geophysics. - Second Edition. Cambridge University Press.

- /VE 02/ VE-Testplan (2001): Ventilation Experiment in Opalinus clay - "VE"
Experiment, Project Deliverable 3, EC contract FIKW-CT2001-00126
- /YAR 89/ Yaramanci, U., Flach, D. (1989b). Entwicklung einer vollautomatischen
Gleichstrom-Geoelektrikanlage für den Einsatz im Vorhaben "Dammbau im
Salzgebirge". GSF-Bericht 1/89.

List of Figures

Figure 1-1	Microtunnel at the Mt. Terri Underground Research Laboratory (URL).....	1
Figure 1-2	Instrumented VE test section in the microtunnel at the Mt. Terri Underground Research Laboratory (URL)	2
Figure 2-1	Principle configuration of a dipole-dipole measurement.....	3
Figure 3-1	RESECS measuring system.....	8
Figure 3-2	Decoder boxes of geoelectric monitoring system.....	9
Figure 3-3	Cross section through electrode borehole.....	11
Figure 4-1	Geoelectric array around the VE microtunnel.....	13
Figure 5-1	BVE sample poured with wax in a plastic tube.....	15
Figure 5-2	Exsiccator with clay samples.....	16
Figure 5-3	Air comparison pycnometer (after Beckman)	17
Figure 5-4	Schematic of the 4-point arrangement for the determination of the resistivity.....	18
Figure 5-5	Measurement set-up for determination of clay rock resistivity.....	19
Figure 5-6	Results of the resistivity measurements at the state of delivery without additional saturation	21
Figure 5-7	Results of the resistivity measurements after saturation and drying	22
Figure 5-8	Combination of the results of the resistivity measurements after saturation and drying, and at the state of delivery without additional saturation	23
Figure 6-1	Geoelectric modelling of a resistivity distribution with a discontinuous desaturated ring of 10 cm width. Left: Input model, right: Inversion result	26
Figure 6-2	Geoelectric modelling of a resistivity distribution with a continuous desaturated zone around the microtunnel. Left: Input model, right: Inversion result	26
Figure 7-1	Resistivity tomograms of the first resaturation phase – September 21, 2002 (upper left), January 22, 2003 (upper right), April 30, 2003 (lower left), and the reduced tomogram of April 30, 2003 (lower right).....	28

Figure 7-2	Resistivity tomograms of the desaturation phase – August 21, 2003 (upper left), September 25, 2003 (upper right), November 16, 2003 (lower left), and January 25, 2004 (lower right)	29
Figure 7-3	Relative change of resistivity during the desaturation phase with respect to the resistivity distribution on August 21, 2003 - September 25, 2003 (upper left), November 16, 2003 (upper right), and January 25, 2004 (lower left). Dark blue = no change, red = increase by a factor of 3	30
Figure 7-4	Resistivity tomograms of the second resaturation phase – January 31, 2004 (upper left), March 31, 2004 (upper right), and May 31, 2004 (lower left).....	31
Figure 7-5	Resistivity evolution at three points in the wall of the micro-tunnel	32
Figure 7-6	Position of the boreholes for the post-test investigations /VE 02/	33
Figure 7-7	Arrangement of the boreholes and position of the samples (n. a.: not available, sample was disturbed)	33
Figure 7-8	Borehole BVE 87 (above) and BVE 88 (below) with side boreholes	35
Figure 7-9	View into a borehole before removal of the core sample	35
Figure 7-10	Two core samples taken from the inclined borehole BVE 88 (depth: 0.15 m - 0.3 m and 0.3 m - 0.44 m).....	36
Figure 7-11	Resistivity measurement results of samples obtained before and after ventilation	37
Figure 7-12	Distribution of the resistivities at the depth from which the samples were taken (n. a.: not available)	38
Figure 7-13	Resistivity of the samples taken after ventilation in dependence of the distance from the borehole wall.....	39

List of Tables

Table 5-1	Geometrical data of the investigated samples of the cores BVE 1/1, BVE 1/2	16
Table 5-2	Bulk densities, porosities, and water contents of the investigated BVE samples; grain density: 2.73 g/cm ³	20
Table 7-1	Geometrical data of the investigated samples of the boreholes BVE 88 and BVE 89; (BVE 89 (2.) I was taken from the side borehole)	34
Table 7-2	Resistivities of Mont Terri VE-samples before and after ventilation; grain density: 2.73 g/cm ³	37

**Gesellschaft für Anlagen-
und Reaktorsicherheit
(GRS) mbH**

Schwertnergasse 1
50667 Köln
Telefon +49 221 2068-0
Telefax +49 221 2068-888

Forschungsinstitute
85748 Garching b. München
Telefon +49 89 32004-0
Telefax +49 89 32004-300

Kurfürstendamm 200
10719 Berlin
Telefon +49 30 88589-0
Telefax +49 30 88589-111

Theodor-Heuss-Straße 4
38122 Braunschweig
Telefon +49 531 8012-0
Telefax +49 531 8012-200

www.grs.de